Diagnosing quark matter by measuring the total entropy and the photon or dilepton emission rates

Rudolph C. Hwa
Institute of Theoretical Science, University of Oregon, Eugene, Oregon 97403-1229

K. Kajantie
Department of Theoretical Physics, Siltavuorenpenger 20 C, 00170 Helsinki, Finland
(Received 1 March 1985)

The rates of thermal emission of photons and lepton pairs from quark matter formed in ultrarelativistic nuclear collisions are related to the conserved total entropy of the quark matter. The transient existence of quark matter can be diagnosed by measuring the entropy separately from particle multiplicities and comparing the predicted and observed rates. The thermal soft-multiple-scattering rates are compared with the direct hard-single-scattering rates. Transverse-momentum effects, the background due to $D\bar{D}\to\mu\bar{\mu}X$ decays, and fluctuations are discussed.

I. INTRODUCTION

Considerable new insight to the problem of dilepton emission[1] from quark matter[2-6] has recently been given by McLerran and Toimela.[7] In particular, these authors have pointed out that for those values of $M_T=(M^2+q_T^2)^{1/2}$ of the pair for which the thermal rate is dominant, the dependence on M_T is powerlike, not an exponential. The purpose of this paper is to consider the thermal rate of dileptons and also of real photons in some more detail and to show that its magnitude can be used to diagnose quark matter in the central region of a collision of two ultrarelativistic nuclei, A and B. The thermal rate can, namely, be expressed in terms of the conserved total entropy squared of the expanding quark matter. When the entropy is independently determined by measuring $dN^{AB\to\pi}/dy_\pi$ we have a realistic quantitative method for diagnosing quark matter: if the calculated and observed rates for $1\lesssim M_T\lesssim 3$ GeV of dileptons agree one has possibly observed quark matter; otherwise some of the assumptions are wrong (e.g., thermalization is not attained or expansion is not adiabatic).

Thermal rates are usually very sensitively dependent on temperature. The point here is that, for sufficiently large temperatures, the rate becomes independent of it. By measuring the pair production rate at fixed M_T or M, or the $\langle q_T\rangle$ of the pair as a function of $dN^{AB\to\pi}/dy_\pi$, A, B, and $\sqrt{s}$, one can check whether sufficient temperatures have been reached to render our theoretical calculations sensible.

While the calculation of the thermal rate involves the physics of very soft QCD processes and is beset with many difficulties, the calculation of direct hard large-mass pair production in pp collisions is one of the successes[8] of perturbative QCD. Of course, there will also be new effects[9] in $AB\to\mu\bar{\mu}$. Where the thermal rate is large (small-M region) the Drell-Yan calculation is not valid any more, but it is still quite interesting to extrapolate the Drell-Yan rate to the small-M region and to compare with the thermal rate. The results will be shown to be very similar; only the sea-quark density at $x=0$ is replaced by a numerical constant times the pion rapidity density at $y_\pi=0$. The similarity is due to the fact that we do not directly "see" quark matter itself; only the asymptotic remnants coming from its decay in both cases.

A background to the small-M region comes from the processes[10,11] $A+B\to D\bar{D}+X\to\mu\bar{\mu}+X'$. This will have to be eliminated to get hold of the pure QCD process discussed here.

Real-photon production[2,12] can be discussed similarly. We shall in the following relate also the thermal rate of producing real photons [at $\simeq 90°$ in the center-of-mass system (c.m.s.) and with $0.6\lesssim q_T\lesssim 2$ GeV] to the total entropy squared and compare with the corresponding extrapolated direct rate. The situation, however, is in this case more complicated both theoretically (quark-mass singularities have to be shielded, higher-order terms may be large) and experimentally (large π^0 background).

II. THE DRELL-YAN RATE

Let us start from the end of the problem, i.e., the Drell-Yan pair production [Fig. 1(a)], which is theoretically under reasonable control: for M and $\sqrt{s}$ large and $0<M/\sqrt{s}<1$ fixed, the rate of $A+B\to\mu\bar{\mu}+X$ can be written in the form

$$\frac{d\sigma}{dM^2dy}=\frac{4\pi\alpha^2}{9M^4}\sum_q e_q^2[x_1q^A(x_1,M^2)x_2\bar{q}^B(x_2,M^2)+(q\leftrightarrow\bar{q})]\,, \tag{1}$$

$x_1=Me^y/\sqrt{s}$, $x_2=Me^{-y}/\sqrt{s}$. More complicated expressions can be written down[8] for $d\sigma/dM^2dy\,d^2q_T$. The difference to the pp case is that structure functions of the nuclei now appear. It is evident that, independent of any interest in quark matter, measurements of $A+B\to\mu\bar{\mu}+X$ at large M will give important new information on the nuclear structure functions and, e.g., shed new light on the European Muon Collaboration (EMC) effect.[9] Here we shall only need the small-$M/\sqrt{s}$ limit of

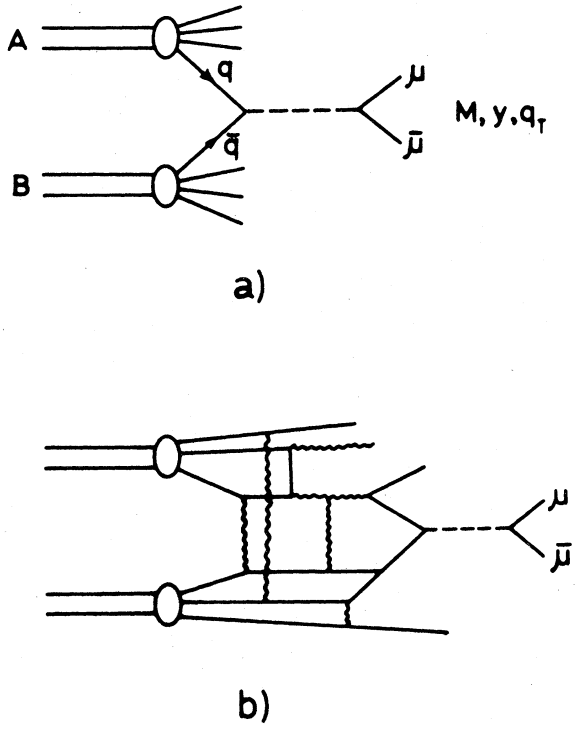

FIG. 1. (a) Drell-Yan pair production. (b) Thermal pair production.

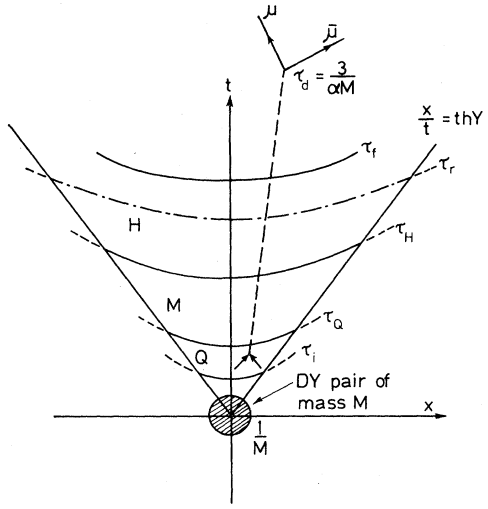

FIG. 2. Longitudinal space-time domain of existence of QCD matter in a nucleus-nucleus collision, Q = quark matter, M = mixed phase, H = hadronic matter, τ_i, τ_Q, τ_H, and τ_f are proper times separating these phases, τ_r (magnitude relative to the other times is uncertain) is the proper time when the transverse rarefaction wave starts disturbing the longitudinal motion, τ_d is the lifetime of the produced pair, and $|x|/t < \tanh Y$ is the range of $|x|/t$ considered.

(1). Concretely, take M as small as possible but still compatible with the factorized form (1) (say, $M \gtrsim 5$ GeV) and s so large that in the structure functions we can effectively take $x_2 = 0$, $x_F = x_1 - x_2 = x_1$ for $y > 0$ (say, $\sqrt{s} \geq 100$ GeV). Let us perform a valence-sea decomposition ($xu^p = 2V + S$, $xd^p = V + S$, etc.), consider $y > 0$ and divide by $\sigma_{\text{in}} = \pi(R_A + R_B)^2$ to obtain the rapidity density. Then, including u,d,s quarks, we have

$$\frac{dN_{\text{DY}}(y \geq 0)}{dM^2 dy} = \frac{4\pi\alpha^2}{9M^4} \frac{1}{\pi(R_A + R_B)^2} \frac{4}{3} S^A(0) S^B(0) \times \left[\frac{S^A(x_F)}{S^A(0)} + \frac{3}{4} \frac{V^A(x_F)}{S^A(0)} \right], \quad (2)$$

where the quantity inside the large parentheses $= 1$ for $x_F = 0$. For values of M smaller than ≈ 5 GeV other contributions, for instance, pairs from thermalized quark matter, will appear.

To compare with quark matter, which exists in an extended region of space-time [Figs. 1(b) and 2], one may also ask what Drell-Yan pair production looks like in space-time. Building in the uncertainty principle to the parton model (small-momentum partons are less well localized) one finds that Drell-Yan pairs are on the average produced at $x = t = 0$ but with an average fluctuation of $1/M$ (Fig. 2) in x and t. For $M \geq 3$ GeV this fluctuation is ≤ 0.06 fm.

III. THE SIMILARITY HYDRODYNAMICAL FLOW

Consider then what happens if quark matter is formed. We shall make the standard assumptions[13] about thermalization, isentropic expansion and similarity flow in the central region.[14,15] The longitudinal space-time region in which quark matter exists is then as shown in Fig. 2. Transversally the region is assumed to be a cylinder of radius R_A (for zero impact parameter, $R_A \leq R_B$); furthermore, under the assumption that the coupling between the longitudinal and transverse flows is weak, transversal variation of all quantities is neglected. The velocity and temperature of the matter then are, for $\tau_i < \tau < \tau_Q$ in the quark phase,

$$v(x,t) = \frac{x}{t} \equiv \tanh\eta \,, \quad (3)$$

$$T^3(\tau)\tau = \frac{1}{4a} \frac{1}{\pi R_A^2} \frac{S}{2Y} \equiv C \,, \quad (4)$$

where the equation of state

$$\rho_q = aT^4 - B \,, \quad B = \text{bag constant} \,,$$
$$s = (\epsilon + p)/T = dp/dT = 4aT^3 \,, \quad (5)$$
$$a = \frac{8\pi^2}{45} + \frac{7}{8}\frac{2\pi^2}{15} N_F = 5.25 \quad (N_F = 3) \,,$$

has been assumed for quark matter, $-Y \leq \eta \leq Y$ is the interval of η we are considering, and S is the total entropy of the flow in this interval. To appreciate the fundamental relation (4) note that, for $v = x/t$,

$$S=\int d^2x_T \int d\sigma^\mu s_\mu = \pi R_A{}^2 \int s(\tau)(t\,dx - x\,dt)/\tau$$
$$= \pi R_A{}^2 \int_{-Y}^{Y} d\eta\, s(\tau)\tau = \pi R_A{}^2 4aT^3(\tau)\tau 2Y \,. \quad (6)$$

To relate S to observables one has to assume that the expansion is adiabatic also through the mixed and hadron phases (Fig. 2), i.e., S is constant. Using the equation of state

$$\rho_h = a_\pi T^4 \,, \quad a_\pi = \frac{\pi^2}{30} \,, \quad (7)$$

for the hadron phase, the critical temperature is

$$T_c = [B/(a-a_\pi)]^{1/4} \,. \quad (8)$$

The remaining flow parameters then are such that the system is in a mixed phase with

$$T = T_c \quad \text{for } \tau_Q < \tau < \tau_H = \frac{a}{a_\pi}\tau_Q \quad (9)$$

and in the hadron phase with

$$T^3(\tau)\tau = \frac{a}{a_\pi}C = \frac{1}{4a_\pi}\frac{1}{\pi R_A{}^2}\frac{S}{2Y} \quad \text{for } \tau > \tau_H \,. \quad (10)$$

Assuming further that the decoupling of pions is adiabatic, S can be measured by

$$\frac{S}{2Y} \approx \frac{dS}{dy_\pi} \approx c\frac{dN^{AB\to\pi}}{dy_\pi}(b=0) \,,$$
$$c = \frac{2\pi^4}{45\zeta(3)} \approx 3.6 \,, \quad (11)$$

where $b=0$ indicates zero impact parameter. The geometrical complication of the $b\neq 0$ case will be discussed in the following. If $2Y$ is the total rapidity range, S is effectively estimated by the total multiplicity. However, one could use the local fluctuations in dN/dy_π and let $2Y$ be the width of the enhanced region. How these local fluctuations leak to adjacent regions is a hydrodynamic problem deserving further study. Anyway one knows that these fluctuations are damped.[16]

By virtue of (11) the initial temperature and time can be related to the hadron distribution in the final phase by (for $T_i > T_c$)

$$T_i{}^3\tau_i = \frac{c}{4a}\frac{1}{\pi R_A{}^2}\frac{dN^{AB\to\pi}}{dy_\pi}(b=0) \,,$$

or

$$\left[\frac{T_i}{100\text{ MeV}}\right]^3 = \frac{1\text{ fm}}{\tau_i}\frac{0.5}{A^{2/3}}\frac{dN^{AB\to\pi}}{dy_\pi}(b=0) \,. \quad (12)$$

The numerical value of T_i, on which some quantitative predictions depend sensitively (see later), is thus only determined in terms of the initial thermalization time τ_i. However, it is to be emphasized that the main quantitative quark-matter diagnostic test is independent of the numerical value of T_i, provided that it is large enough.

T_i will depend on the four experimentally controllable and detectable quantities $\sqrt{s}$, A, B, and dN/dy_π. Equation (12) is useful only if τ_i depends on these only relatively weakly. In Ref. 7 it is argued that $\tau_i = \tau_p/A^\delta$, $0<\delta<\frac{1}{3}$, where $\tau_p = 0.5$ fm is the formation time determined, e.g., from pA collisions.

Numbers are quite uncertain, but, for illustration, a possible set of them is as follows. Specify first the equation of state by $T_c = 160$ MeV, a and a_π as in (5) and (10). Consider a $^{16}O+$ heavier target collision with $dN^\pi/dy_\pi = 42$. Then the initial parameters could be $\tau_i = 0.1$ fm, $T_i = 320$ MeV, $\epsilon_i = 17$ GeV/fm^3. The quark phase would end and the mixed phase start at $\tau_Q = 0.8$ fm, $T_c = 160$ MeV, $\epsilon_Q = 1.4$ GeV/fm^3, the mixed phase would last until $\tau_H = 9.8$ fm, $T_c = 160$ MeV, $\epsilon_H = 0.1$ GeV/fm^3, and the hadron phase until $\tau_f = 14$ fm, $T_f = m_\pi = 140$ MeV, $\epsilon_f = 12 m_\pi{}^4$. The spectacularly long lifetime of the mixed phase (for $N_F = 2$ it would be from 0.8 to 9.8 fm) is conceivable, since $v_{\text{sound}} = 0$ in the mixed phase and the transverse rarefaction wave does not propagate; only the longitudinal expansion reduces the energy density from ϵ_Q to ϵ_H. In the hadron phase the transverse rarefaction wave again propagates with $v_{\text{sound}}{}^2 = \frac{1}{3}$ and soon spoils the longitudinal-similarity-flow pattern.

IV. DILEPTONS FROM THERMAL EMISSION AS QUARK-MATTER DIAGNOSTICS

To calculate the thermal rate one should fold the rest-frame rate over the space-time history (Fig. 2) of the system. In the quark phase the rest-frame rate is (with Maxwell-Boltzmann statistics, for simplicity)

$$\sum e_q{}^2 \frac{\alpha^2}{8\pi^4} e^{-E/T} \,. \quad (13)$$

The rate from the hadron phase is more complicated to calculate,[4] due to unknown form-factor effects. However, in the mixed phase T stays constant at $T = T_c$ and the change in T during the hadron phase is likely to be very small. Also the longitudinal similarity flow will be disrupted by the transverse flow for all but the largest nuclei. We can thus parametrize the rate from the mixed and hadron phases by constant $\times e^{-E/T_c}$: the interesting new physics will reside in nonexponential terms.

The detailed inclusion of transverse-coordinate effects in the calculation would be a very complex affair. In the spirit of the central-region similarity solution we shall assume that no quantities depend on x_T. Since the average rate per collision (averaged over all impact parameters) $\langle N(b)\rangle$ has a geometrical factor

$$(\pi R_A{}^2)(\pi R_B{}^2)/\pi(R_A+R_B)^2 \,,$$

while the rate at $b=0$ is proportional to $\pi R_A{}^2$ for $A \leq B$, the ratio $\langle N(b)\rangle/N(0)$ is $1/(1+R_A/R_B)^2$. On the other hand, the same geometrical consideration also gives the result that the height of the rapidity plateau dN/dy_π at zero impact parameter is $(1+R_A/R_B)^2$ times the observed dN/dy_π, averaged over all b.

The space-time integration is now carried out by using Eqs. (4) and (11) to derive

$$\int d^2x_T dt\, dx = \pi R_A{}^2 \int_{\tau_i}{}^{\tau_f} d\tau\, \tau \int_{-Y}^{Y} d\eta$$
$$= \pi R_A{}^2 \left[\frac{c}{4a} \frac{1}{\pi R_A{}^2} \frac{dN}{dy_\pi}(b=0) \right]^2 \int_{T_Q}{}^{T_i} dT \frac{3}{T^7} \int_{-Y}^{Y} d\eta \ .$$

This is the key point at which the square of the entropy [related to $(dN/dy_\pi)^2$] enters. Note also how one $\pi R_A{}^2$ cancels to give $1/\pi R_A{}^2$. For $R_A < R_B$ one does not automatically get $1/\sigma_{\rm in}$, $\sigma_{\rm in} = \pi(R_A + R_B)^2$. Hydrodynamics only knows about the larger R via T_i.

The thermal rate, averaged over all b, then gets a factor $(1+R_A/R_B)^{-2}$ from the average over b and a factor $(1+R_A/R_B)^4$ from relating $(dN/dy_\pi)^2$ at $b=0$ to the average over b. The result, including u,d,s quarks, is

$$\frac{dN_{\rm th}^{AB\to\mu\bar{\mu}}}{dM^2 dy\, d^2q_T} = \frac{\alpha^2}{12\pi^4} \frac{(1+R_A/R_B)^2}{\pi R_A{}^2} \left[\frac{c}{4a} \frac{dN^{AB\to\pi}}{dy_\pi} \right]^2$$
$$\times \int_{-Y}^{Y} d\eta \left[\int_{T_c}{}^{T_i} dT \frac{3}{T^7} \exp\left[-\frac{1}{T} M_T \cosh(y-\eta) \right] + \frac{\lambda}{T_c{}^6} \exp\left[-\frac{1}{T_c} M_T \cosh(y-\eta) \right] \right] , \tag{14}$$

where the first term represents the quark phase and the second the mixed and hadron phases and λ is a constant. Note that dN/dy_π in Eq. (14) is now the observed height, not that at $b=0$. Assuming that the rest-frame rate from the hadron fluid is also given by Eq. (13), we have

$$\lambda = \frac{1}{2} \left[\frac{a^2}{a_\pi{}^2} - 1 \right] \approx 125 \ . \tag{15}$$

Remember also that T_i depends on dN/dy_π according to Eq. (12).

The η range contributing to (14) is $y - (T/M_T)^{1/2} \le \eta \le y + (T/M_T)^{1/2}$. In all relevant cases $T/M_T \ll 1$ and for centrally produced pairs ($y \ll Y$) the η integral can be carried out using a quadratic approximation of $\cosh(y-\eta)$ (Ref. 7) [more precisely, the result is $K_0(M_T/T)$]:

$$\frac{dN_{\rm th}^{AB\to\mu\bar{\mu}}}{dM^2 dy\, d^2q_T} = \frac{4\pi\alpha^2}{9} \frac{9\sqrt{2\pi}\Gamma(5.5)}{16\pi^5} \frac{(1+R_A/R_B)^2}{\pi R_A{}^2} \left[\frac{c}{4a} \frac{dN^{AB\to\pi}}{dy_\pi} \right]^2$$
$$\times \left\{ \frac{1}{M_T{}^6} \left[P\left[5.5, \frac{M_T}{T_c}\right] - P\left[5.5, \frac{M_T}{T_i}\right] \right] + \frac{\lambda}{3\Gamma(5.5) T_c{}^6} \left[\frac{T_c}{M_T} \right]^{1/2} e^{-M_T/T_c} \right\} , \tag{16}$$

where (Fig. 3)

$$P(z,a_c) - P(z,a_i) = \frac{1}{\Gamma(z)} \int_{a_i}{}^{a_c} dt\, t^{z-1} e^{-t} \ . \tag{17}$$

From this one calculates

$$\langle q_T \rangle = \frac{32}{35\sqrt{2}} M \frac{P\left[4, \frac{M}{T_c}\right] - P\left[4, \frac{M}{T_i}\right] + \frac{\lambda}{18} \left[\frac{M}{T_c} \right]^4 e^{-M/T_c}}{P\left[4.5, \frac{M}{T_c}\right] - P\left[4.5, \frac{M}{T_i}\right] + \frac{16\lambda}{315\sqrt{\pi}} \left[\frac{M}{T_c} \right]^{4.5} e^{-M/T_c}} , \tag{18}$$

$$\langle q_T{}^2 \rangle = \tfrac{4}{7} M^2 \frac{P\left[3.5, \frac{M}{T_c}\right] - P\left[3.5, \frac{M}{T_i}\right] + \frac{8\lambda}{45\sqrt{\pi}} \left[\frac{M}{T_c} \right]^{3.5} e^{-M/T_c}}{P\left[4.5, \frac{M}{T_c}\right] - P\left[4.5, \frac{M}{T_i}\right] + \frac{16\lambda}{315\sqrt{\pi}} \left[\frac{M}{T_c} \right]^{4.5} e^{-M/T_c}} , \tag{19}$$

and

$$\frac{dN_{\rm th}^{AB\to\mu\bar{\mu}}}{dM^2 dy} = \frac{4\pi\alpha^2}{9} \frac{945}{128\pi^3} \frac{(1+R_A/R_B)^2}{\pi R_A{}^2} \left[\frac{c}{4a} \frac{dN^{AB\to\pi}}{dy_\pi} \right]^2$$
$$\times \left\{ \frac{1}{M^4} \left[P\left[4.5, \frac{M}{T_c}\right] - P\left[4.5, \frac{M}{T_i}\right] \right] + \frac{16\lambda}{315\sqrt{\pi}} \frac{1}{T_c{}^4} \left[\frac{M}{T_c} \right]^{1/2} e^{-M/T_c} \right\} . \tag{20}$$

For $M \gg 4.5T_i$ this behaves like

$$\frac{dN_{\rm th}^{AB\to\mu\bar{\mu}}}{dM^2dy} = \frac{4\pi\alpha^2}{9M^4}\cdot\frac{9}{8}\cdot\frac{(1+R_A/R_B)^2}{\pi {R_A}^2}\left[\frac{c}{4a}\frac{dN^{AB\to\pi}}{dy_\pi}\right]^2\left[\frac{M}{\pi T_i}\right]^{7/2} e^{-M/T_i} . \tag{21}$$

The previous results hold in the central region $y \ll Y$ and are independent of y. If we arbitrarily cut off the flow for $|y| > Y$, the dependence of the quark-matter rate on $Y-y$ becomes

$$\tfrac{1}{2}+\tfrac{1}{16}[3\tanh^5(Y-y)-10\tanh^3(Y-y) +15\tanh(Y-y)] . \tag{22}$$

This factor is normalized to 1 at $y=0$, $Y \gg 1$ and, if Y is taken to be the beam c.m.s. rapidity Y_B, Y_B-y in it can be related to the Feynman x_F by $x_F = e^{y-Y_B}$ (normalizing $y=Y_B$ to $x_F=1$). Of course, the similarity flow is not valid near $|\eta| = Y_B$ and the result (22) is only a qualitative illustration of how thermal processes can send pairs to $x_F > 1$.

The diagnosis of quark matter on the basis of the above formulas now proceeds as follows. The experimental quantity being analyzed is the dilepton rate measured in $A+B$ collisions as a function of $M(\gtrsim 1$ GeV), $y(\approx 0)$, q_T, A, B, $\sqrt{s}$, and the associated dN/dy_π.

(1) One starts from the large-M ($\gtrsim 5$ GeV) end and verifies as in pp collisions the validity of the Drell-Yan picture using the functions $q^A(x,M^2)$ measured in deep inelastic scattering. When approaching the smaller-M range a component not described by the direct Drell-Yan mechanism is identified. The background from $A+B\to D\bar{D}+X\to\mu\bar{\mu}+X$ to this component has to be eliminated.

(2) In the $M \lesssim 3$ GeV range one checks that the rate [Eq. (16)] as a function of M and q_T only depends on M_T and identifies the values of M_T for which the $\exp(-M_T/T_c)$ term is negligible. The general structure of the two terms in (16) is apparent from Figs. 3 and 4. The quark-matter term is powerlike for $T_c \lesssim M_T/5.5 \lesssim T_i$ (Ref. 7 and Fig. 3) and vanishes like $\exp(-M_T/T_i)$ for $M_T \gg 5.5T_i$. The crucial parameter is thus T_i: it should be large enough so that the quark-matter term separates from the $\exp(-M_T/T_c)$ term before being buried under the Drell-Yan term at large M_T (Sec. IV). T_i will increase monotonically with dN/dy_π, A, B, and $\sqrt{s}$. Note how the rate at fixed M_T in Fig. 4 becomes independent of T_i when T_i is large enough.

(3) To separate the quark-matter term one may also use the zeroth [Eq. (20)], first [Eq. (18) and Figs. 5(a) and 5(b)] and second [Eq. (19)] moments over q_T. The exponential and quark-matter terms give

$$\langle q_T\rangle = \begin{cases} \left[\frac{\pi}{2}MT_c\right]^{1/2}, & T_c \ll M \text{ , exponential} \\ 0.645M, & 4T_c \lesssim M \lesssim 4T_i \text{ , quark matter ;} \end{cases} \tag{23}$$

the exact expression interpolates between these. In practice, one plots $\langle q_T\rangle$ as a function of the associated dN/dy_π for various M ($1 \lesssim M \lesssim 3$ GeV) and checks that the increase of $\langle q_T\rangle$ as a function of dN/dy_π is faster the larger M is, in a way which is compatible with the expressions above.

Note that this mechanism of increasing $\langle q_T\rangle_{\mu\bar{\mu}}$ is different from that proposed[17–19] for increasing $\langle q_T\rangle_\pi$ as a function of dN/dy_π: the former is a thermometer while the latter is a barometer,[20] sensitive to the hydrodynamical flow caused by the pressure difference between quark matter and outside vacuum.

(4) After the quark-matter term has been identified with normalization-independent tests, the existence of adiabatically expanding quark matter is diagnosed by verifying that the magnitude of the rate agrees with the prediction (16). Note that this prediction does not depend on

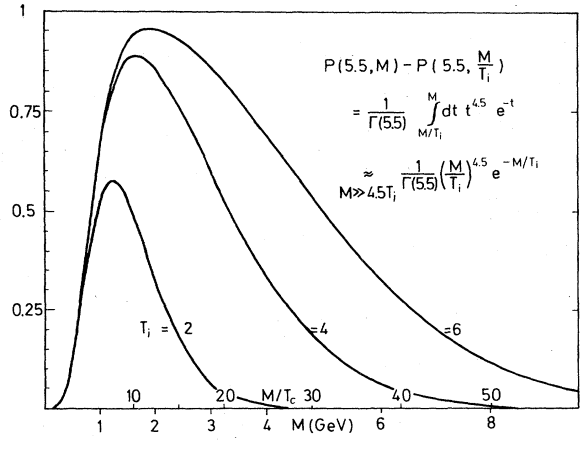

FIG. 3. A plot of the integral appearing in Eq. (16), M and T_i are in units of T_c. Whenever magnitude in GeV units is given, $T_c = 160$ MeV is used here and in later figures.

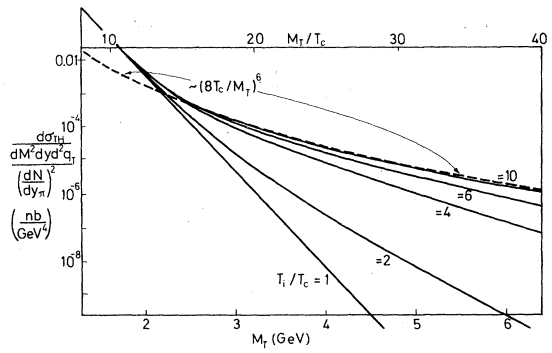

FIG. 4. A plot of the cross section for thermal pair production in $A+A$ [Eq. (16) multiplied by $\sigma_{\rm in}=4\pi {R_A}^2$], divided by the associated pion rapidity density squared as a function of M_T for various T_i. The very uncertain magnitude of the $\exp(-M_T/T_c)$ term is fixed by using Eq. (15); this term is given by $T_i = T_c$. Note how the prediction saturates when T_i is increased at fixed M_T.

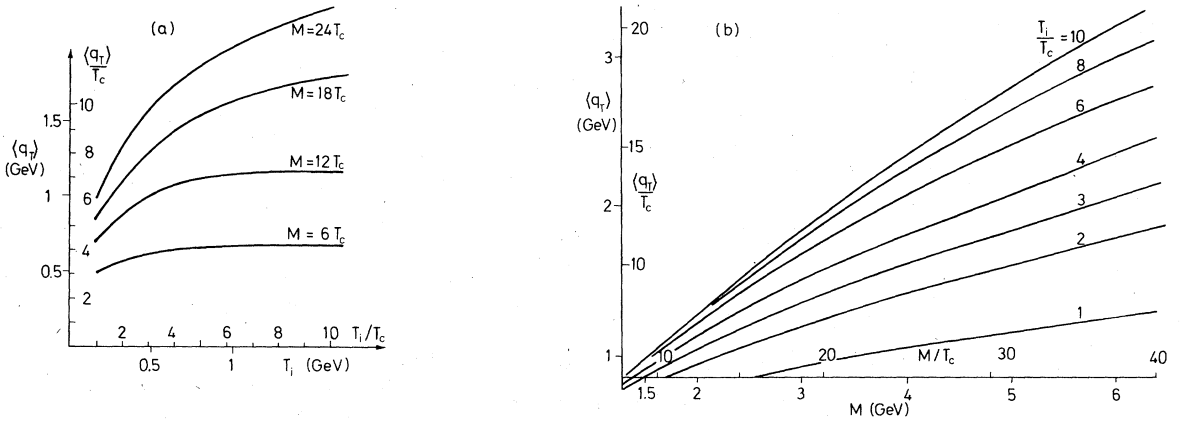

FIG. 5. Plot of $\langle q_T \rangle$ [Eq. (18) with $\lambda=0$] as a function of (a) T_i for various M, (b) M for various T_i. The values of $\langle q_T \rangle$ for $T_i=T_c$ correspond to the $\exp(-M/T_c)$ term.

T_i, provided that it is large enough. Also the numerical values of a and c given in Eqs. (5) and (11) are expected to be more reliable for $T \gg T_c$; large T_i also helps to reduce the uncertainty of the result due to the uncertainty concerning these parameters. If agreement is found over a wide range of the variables considered, the case for quark matter is strong. If not, there are many possible reasons for the disagreement: (i) The expansion is not adiabatic. (ii) The simple equation of state (5), (10) is incorrect. (iii) The effects if transverse variation are important. (iv) The background from $AB \to D\bar{D}X \to \mu\mu X$ is large.[10,11] (v) Quark matter does not exist.

The use of a similarity solution implies a neglect of fluctuations in dN/dy_π. Existing cosmic-ray data indicate that there are sizable fluctuations even in $A+B$ collisions. Dilepton measurements will help to find out at what stage these fluctuations arise. If the fluctuations are formed by the initial quantum processes, they exist at τ_i and one expects a positive correlation between the lepton and pion rates (although the fluctuations are damped by hydrodynamics). If the fluctuations are formed by later macroscopic processes, e.g., by bubbles nucleated in the course of the phase transition, one expects little correlation.

V. RELATION BETWEEN THE DRELL-YAN AND THERMAL RATES

Physically we expect that the Drell-Yan and thermal rates dominate in different parts of the phase space: the former is a single-collision momentum-space leading-twist mechanism, the latter a multiple-collision coordinate-space higher-twist mechanism. However, we can still gain some interesting insight to the problem by comparing them in various parts of the phase space.

Note first the scaling rules

$$\frac{d\sigma_{\rm th}(y=0)}{dM^2dy} = \frac{1}{M^4} F\left[\frac{M}{T_i}\right],$$

$$\frac{d\sigma_{\rm DY}(y=0)}{dM^2dy} = \frac{1}{M^4} G\left[\frac{M}{\sqrt{s}}, \ln\frac{M^2}{Q_0^2}\right],$$

where F and G have been given explicitly. Both demand $M \gg T_c \sim m_\mu$; in the Drell-Yan case one has a direct control over the variable $\sqrt{s}$ while this is not so for T_i.

Consider then $M \lesssim 3$ GeV, $M/\sqrt{s} \ll 1$, A, B, and dN/dy_π so large that $T_i \gtrsim M/5.5$ and such that the $\exp(-M/T_c)$ term in (20) is negligible. Then both the Drell-Yan (DY) [Eq. (2)] and thermal (th) [Eq. (20)] rates are (for $|y| \ll Y$) $dN/dM^2dy = \text{constant}/M^4$, where the constants are related by

$$S^A(0)S^B(0) \text{ in DY} \to \left[0.10\frac{(R_A+R_B)^2}{R_AR_B}\frac{dN^{AB\to\pi}}{dy_\pi}\right]^2 \text{ in th .} \quad (24)$$

The number 0.10 is actually $(2835/512\pi^3)^{1/2}\,(c/4a)$. The R-dependent factors arise from two sources: the geometric correction transforming $b=0$ to an average over b and the fact that the entropy relation (6) only contains R_A (R_B is hidden in T_i). This correction factor is 16 for $R_A=R_B$ and goes like R_B^2/R_A^2 for small R_A, provided that A is large enough to justify (14) for thermalized quark matter.

Numerically, neglecting nuclear effects,[9] one expects that $S^A(0) \approx AS^p(0) \approx 0.2A$. Taking $A=B$, for $dN^{AA\to\pi}/dy_\pi$ the model in Ref. 21 gives $\approx 0.4A\rho_0$ and in Ref. 22 $\approx A\rho_0$ ($\rho_0=3$ is the pp rapidity density at $\sqrt{s} \approx 30$ GeV). For average events in these models the observed thermal rate is an order of magnitude higher than the extrapolated Drell-Yan rate. A consideration of the estimate (12) for the initial temperature (with $\tau_i = 0.5\ \text{fm}/A^\delta$, $\delta = 0, \frac{1}{3}$) shows that the average events in these models may perhaps not produce $T_i \gtrsim 2T_c$ required for fully developed quark matter. When one considers only events with large dN/dy_π, the thermal pair production rate should dominate.

The enhancement of small-mass lepton pairs has been considered earlier[23–25] for pp collisions. The difference now is that there is a well-defined framework for calculating the low-mass ($M \gtrsim 1$ GeV) rate and correlating it with other measured quantities. In addition, there is an important source of background contributing at small M, that from $A+B \to D\bar{D}+X \to \mu\bar{\mu}+X'$ (Ref. 10). This back-

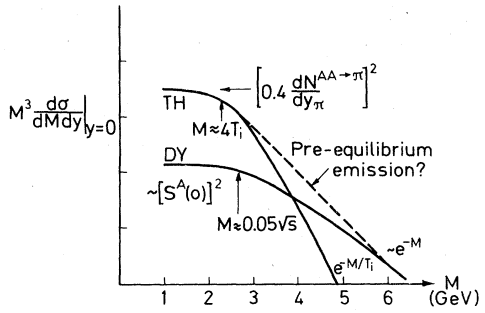

FIG. 6. Comparison of thermal and extrapolated Drell-Yan pair production rates.

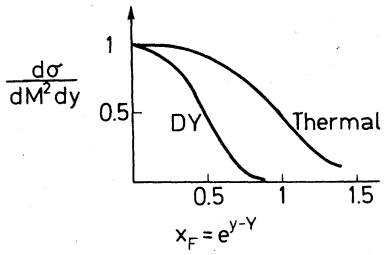

FIG. 7. The x_F dependences of the Drell-Yan and thermal (qualitatively) rates.

ground decreases rapidly with M ($\sim e^{-(2-3)M}$) and the experimentally observed small-M enhancement in pp data arises possibly entirely from this background.[11] For quark-matter diagnostics it is thus important either to know this background, or to avoid it by going to as large a value of M as possible ($M \gtrsim 2$ GeV).

Second, consider what happens if we increase M beyond $4T_i$. Then

$$\tfrac{1}{2}M^3 \frac{d\sigma(y=0)}{dM\,dy} = F\left(\frac{M}{T_i}\right) \sim \left[\frac{M}{T_i}\right]^{7/2} e^{-M/T_i}, \quad \text{th},$$

$$= G\left(\frac{M}{\sqrt{s}}\right) \sim \left[\frac{M}{\sqrt{s}}\right]^{3/2} e^{-25M/\sqrt{s}},$$

DY (Ref. 26). (25)

Both decrease exponentially (this form of the Drell-Yan scaling function is, of course, only approximate) but the decrease of the thermal rate is much faster for energies considered here ($\sqrt{s} \gtrsim 20$ GeV). Although some increase of T_i with $\sqrt{s}$ may be expected, the dominance of the Drell-Yan contribution is clearer with increasing $\sqrt{s}$. The general situation is illustrated in Fig. 6, for the class of events containing quark matter. In the transition region one expects pre-equilibrium emission. To understand this one has to understand the thermalization process.

Finally, one may also qualitatively consider the x_F distribution. If Y in Eq. (14) is taken to be $\ln(\sqrt{s}/M)$ (=c.m.s. beam rapidity), then $x_F = 2q_L/\sqrt{s} = e^{y-Y}$. The x_F distribution (22) of thermal dilepton pairs following from (14) is compared with that of Drell-Yan pairs [Eq. (2)] in Fig. 7. The qualitatively interesting feature with the thermal pairs is that they will also appear beyond the kinematic limit[5] $x_F = 1$. Quantitatively, however, the computation has to be modified: the similarly solution (3) and (4) is not valid in the fragmentation regions and it cannot arbitrarily be cut at $\eta = Y$. Nuclear effects will also lead to an $x > 1$ component in $q^A(x, M^2)$. To identify quark-matter effects at $x_F > 1$ one thus has to check that they cannot be reproduced by the factorized form (1), with the structure functions taken from deep-inelastic-scattering measurements on nuclei.

VI. REAL PHOTONS

Consider then real-photon emission at around 90° in c.m.s. in an $A+B$ collision. At very large q_T ($q_T > 10$ GeV) the production is dominated by the QCD diagrams in Fig. 8. The Compton graph gives the rate

$$\frac{d\sigma^c(y=0)}{dy\,d^2q_T} = \frac{1}{6}\frac{2\alpha\alpha_s}{s^2 \frac{1}{2}x_T} \int_{x_T/(2-x_T)}^1 \frac{dx_1}{x_1 - \frac{1}{2}x_T} \left[F_2^A(x_1) G^B(x_2) \frac{x_2^2 + (\frac{1}{2}x_T)^2}{x_1^2 x_2^3} + G^A(x_1) F_2^B(x_2) \frac{x_1^2 + (\frac{1}{2}x_T)^2}{x_1^3 x_2^2} \right], \quad (26)$$

where

$$x_2 = \frac{x_T x_1}{2 - x_1}, \quad x_T = \frac{2q_T}{\sqrt{s}},$$

$$F_2(x) = x \sum e_q^2 [q(x) + \bar{q}(x)], \quad G(x) = xg(x).$$

Scale breaking in the structure function (not explicitly shown) depends on q_T^2/Q_0^2. The formula for the the annihilation graph (small for pp, important for $\bar{p}p$) is very similar. These two graphs are the only ones of order α_s. They contain that part of the $O(\alpha_s^2)$ bremsstrahlung graph in which the gluon is near-mass shell. The part corresponding to the quark-mass singularity is calculated by summing over the QCD subprocesses producing a quark and letting the quark fragment into a photon. The summation is accurately carried out by using an effective structure function[27–29] and the result is

$$\frac{d\sigma^{\rm br}(y=0)}{dy\,d^2q_T}=\frac{\alpha\alpha_s^2}{2\pi s^2}\ln\frac{q_T^2}{\Lambda^2}\frac{1}{x_T}\times\int_{x_T}^1 dy_T\frac{1}{(\frac{1}{2}y_T)^2}\left[1+\left[1-\frac{x_T}{y_T}\right]^2\right]\times\int_{y_T/(2-y_T)}^1\frac{dx_1}{x_1-\frac{1}{2}y_T}\left[F_2^A(x_1)[G^B(x_2)+\tfrac{4}{9}Q^B(x_2)]\frac{x_1^2+(\frac{1}{2}y_T)^2}{x_1^4}+(x_1\leftrightarrow x_2,A\leftrightarrow B)\right],\quad(27)$$

where

$$x_2=\frac{y_Tx_1}{2-y_T},\quad Q(x)=x\sum[q(x)+\bar{q}(x)]\,.$$

A complete calculation of the finite $O(\alpha_s^2)$ corrections has been presented in Ref. 30. Note that, counting logarithms, Eq. (27) is also of order α_s.

The rates (26) and (27) can be evaluated to the extent the structure functions are known; their magnitudes also depend on the scale factors used. We are interested in (26) and (27) for as small values of q_T as possible (say, down to 3 GeV) and even want to extrapolate beyond that to compare with the thermal rate. Let us choose $\sqrt{s}$ so large ($\sqrt{s}\gtrsim 100$ GeV) that the structure functions in (26) and (27) are probed at $x=0$ ($x_1,x_2\leq x_T$) so that their variation can be neglected. Then the integrals can be easily carried out; the leading terms at small x_T are (including $q\bar{q}\to\gamma g$, $N_F=3$)

$$\frac{d\sigma^{C+\rm ann}(y=0)}{dy\,d^2q_T}=\frac{\alpha\alpha_s}{q_T^4}\frac{7}{27}[G^A(0)S^B(0)+S^A(0)G^B(0)+\tfrac{64}{21}S^A(0)S^B(0)]\,,\quad(28)$$

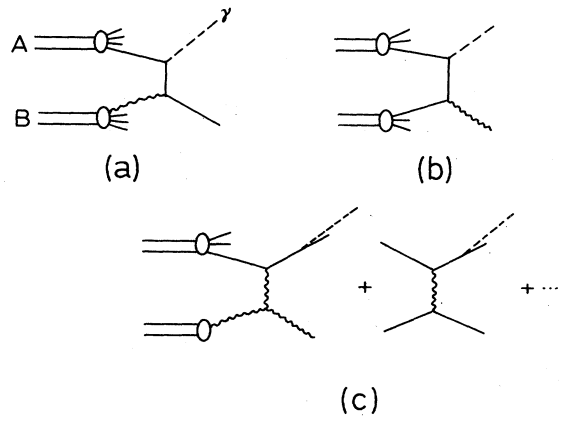

FIG. 8. Diagrams contributing to photon production (a) Compton, (b) annihilation, (c) bremsstrahlung (with quark fragmenting into the photon).

$$\frac{d\sigma^{\rm br}(y=0)}{dy\,d^2q_T}=\frac{\alpha\alpha_s^2}{\pi q_T^4}\ln\frac{q_T^2}{\Lambda^2}\left[\ln\frac{2}{x_T}-\frac{7}{4}\right]\times\tfrac{8}{9}[G^A(0)S^B(0)+S^A(0)G^B(0)+\tfrac{16}{3}S^A(0)S^B(0)]\,.\quad(29)$$

The bremsstrahlung contribution dominates approximately by a factor $1.6[\ln(1/x_T)-1.1]$ over the sum Compton + annihilation. At larger x_T ($\gtrsim 0.1$) bremsstrahlung is smaller.

Consider then thermal emission of real photons with $q_T\gtrsim 1$ GeV at $y=0$ in an $A+B$ collision. The calculation can again be divided in two parts: (1) calculation of the rate of emission from a stationary plasma, (2) folding over the similarity flow in Sec. III.

The diagrams contributing to the spectral emissivity of photons of energy ω are the same as in Fig. 8. Their calculation, even for QED plasmas, is a difficult task.[31] At high temperatures the processes have sharp forward and backward peaks, corresponding to gluon- and quark-mass singularities. These are screened by finite-temperature matter effects.

Consider first the Compton and annihilation graphs. Assuming Maxwell-Boltzmann statistics, using an approximate result for the differential rate derived for $e^+e^-\to\gamma\gamma$ (Ref. 31) and normalizing to the integrated rate, we have

$$\omega\frac{dN_{\rm th}^{c+\rm ann}}{d^3q\,d^4x}=\frac{4\alpha\alpha_s}{\pi^4}T^2\left[\ln\left[\frac{6}{\pi\alpha_s}\frac{\omega}{T}\right]-1-\gamma_E\right]e^{-\omega/T}\,,\quad(30)$$

where $\gamma_E=0.577$ and the quark mass has been replaced by an effective quark mass[32,33] $m_q^2=\frac{1}{6}g_s^2T^2$.

The logarithm in (30) is accurate near $\omega=T$, where $dN/d\omega$ is maximal. It requires that $\omega>O(g_s^2T)$. Actually kinematically $\omega>\frac{1}{2}m_q=O(g_sT)$. Note that, due to electromagnetic damping, anyway only photons with $\omega^2>\frac{1}{6}\sum e_q^2e^2T^2$ or $\omega>0.14T$ propagate. The dispersion relation for transverse oscillations is, namely, $\omega_T^2=k^2+\frac{3}{2}\omega_p^2$, where $\omega_p^2=\frac{1}{3}m_{\rm el}^2=\frac{1}{9}e^2T^2$.

The bremsstrahlung rate[31,34] $dN/d\omega$ has a $1/\omega$ peak. Apart from a constant $O(1)$, it is thus obtained from (30) by multiplying by T^2/ω^2 and replacing the logarithm by $\ln(1/\alpha_s)$. Keeping $\omega\approx g_T$ fixed, T will span a range of

values from T_i to T_c on both sides of ω. Thus initially bremsstrahlung will dominate and finally Compton and annihilation. For $q_T > 1.5\ T_c$ the system will effectively stay longer at lower T and Compton + annihilation will dominate (see below).

The integration over the similarity flow can be carried out exactly as before. The result for Compton + annihilation is

$$\frac{d\sigma_{\rm th}^{c+\rm ann}(y=0)}{dy\,d^2q_T} = \frac{\alpha\alpha_s}{{q_T}^4}\frac{4\sqrt{2\pi}\Gamma(3.5)}{\pi^4} \times \left[\frac{(R_A+R_B)^2}{R_A R_B}\frac{c}{4a}\frac{dN}{dy_\pi}\right]^2 \times \ln\frac{2}{\alpha_s}\left[P\left[3.5,\frac{q_T}{T_c}\right]-P\left[3.5,\frac{q_T}{T_i}\right]\right]. \tag{31}$$

For bremsstrahlung the 3.5 is changed to 1.5 (since the T dependence is T^4) and the numerical factor may be slightly different.

The behavior of the difference $P-P$ in Eq. (31) is similar to that shown in Fig. 3: this difference is between 0.4 and 1 for $3.5\ T_c \lesssim q_T \lesssim 3.5T_i$ (taking $T_i \geq 2T_c$) and decreases exponentially for $q_T \gg 3.5T_i$. Similar statements hold for the bremsstrahlung contribution with 3.5 replaced by 1.5. For $q_T \gtrsim 1.5T_c$ we thus expect Compton + annihilation to dominate. Also large-x_T direct production was dominated by these same diagrams.

We have now two nonoverlapping predictions for the 90° real-photon production cross section: the direct production predictions (26) and (27) hold for $q_T \gtrsim 5$ GeV [and the simplified forms (28) and (29) further demand $\sqrt{s} \gtrsim 100$ GeV]; the thermal prediction (31) holds for $q_T > 3.5T_c$ and gives an exponentially damped rate beyond $q_T = 3.5T_i$, which quite probably is less than 5 GeV. One observes that again (28), (29), and (31) are very similar in form: the product of structure functions in the direct production is replaced by the entropy squared [or $(dN/dy_\pi)^2$] of the expanding quark matter. As with virtual photons the thermal rate will dominate over the extrapolated direct rate only for fairly large values of dN/dy_π.

The diagnosis of quark matter with real-photon measurements could now proceed as follows. First agreement with the direct production QCD prediction is verified at $q_T \gtrsim 5$ GeV. For this one needs independently measured nuclear structure functions. The measurements are then extended to lower q_T and a component not reproducible with nuclear structure functions is identified. In this region the rate should be in agreement with the prediction (31), improved with a more accurate treatment of the bremsstrahlung contribution. For this one needs an independent measurement of dN/dy and a control of the fact that T_i is large enough. The procedure is thus very similar to what was done with virtual photons.

VII. CONCLUSIONS

We have discussed a concrete quantitative method for diagnosing quark matter by measuring the total entropy and the real- or virtual-photon (dilepton) emission rate. The method is based on the following assumptions.

(1) Quark matter is formed in local thermal equilibrium at temperature T_i at proper time τ_i.

(2) The quark-matter equation of state is that of an ideal gas of massless quarks and gluons plus a bag constant term representing the effect of interactions.

(3) The expansion is adiabatic through all stages and follows the central region similarity flow.

(4) Transverse variation up to a radius R_A is neglected. Experimentally one measures the constant of motion of the expansion, the entropy, by measuring the associated pion multiplicity. The real-photon or -dilepton rate is then predicted as a function of T_i. For sufficiently large T_i and for the range $T_c \ll M_T/5.5 \ll T_i$ of dilepton transverse masses[7] the prediction becomes independent of T_i, similarly for real photons. Quark matter is then diagnosed by comparing the measured with the predicted real-photon or -dilepton rates. To apply this test one must eliminate all the backgrounds, for instance, that from $A+B \to D\bar{D}+X \to \mu\bar{\mu}+X'$.

The essential assumption in the above is the one concerning thermalization with $T=T_i$ at τ_i. Without this one cannot even talk about quark matter. At present the theoretical understanding of thermalization is very preliminary[35,36] and the understanding of T_i and τ_i is entirely phenomenological. The main goal of the first experiments is to verify assumption (1); the others only give corrections.

A related question is that of connecting thermal and Drell-Yan pair emission. Large-mass Drell-Yan pair production takes place via a single-pair annihilation in a space-time region of magnitude $1/M$ and is theoretically under good control. If there is thermalization, the thermal rate is also simply calculable. In fact, we have shown that both the thermal and Drell-Yan rates are formally very similar and are related to each other by a simple substitution of renormalization factors; the same holds for the direct and thermal real-photon rates. In between lies the so far unknown pre-equilibrium region. A study of this region, together with the study of fluctuations, is an important topic of further research.

ACKNOWLEDGMENTS

We thank G. Baym, B. Friman, L. Kluberg, L. McLerran, V. Ruuskanen, R. Salmeron, and D. Soper for discussions. The work of R.C.H. was supported in part by the U.S. Department of Energy under Contract No. DE-AT06-16ER10004. He also wishes to thank the Research Institute for Theoretical Physics at the University of Helsinki for its hospitality in the summer of 1984 when this work was initiated.

[1]E. L. Feinberg, Nuovo Cimento **34A**, 39 (1976).
[2]E. Shuryak, Phys. Lett. **78B**, 150 (1978); Yad. Fiz. **28**, 796 (1978) [Sov. J. Nucl. Phys. **28**, 1548 (1978)].
[3]E. Shuryak, Phys. Rep. **61**, 71 (1980).
[4]G. Domokos and J. Goldman, Phys. Rev. D **23**, 203 (1981); G. Domokos, *ibid.*, **28**, 123 (1983).
[5]K. Kajantie and H. I. Miettinen, Z. Phys. C **9**, 341 (1981); **14**, 357 (1982).
[6]S. A. Chin, Phys. Lett. **119B**, 51 (1982).
[7]L. D. McLerran and T. Toimela, Phys. Rev. D **31**, 545 (1985).
[8]G. Altarelli, R. K. Ellis, and G. Martinelli, Phys. Lett. **151B**, 457 (1985).
[9]For a review of the EMC effect, see S. J. Wimpenny, Report No. CERN-EP/84-115 (unpublished); H. Satz, Bielefeld Report No. BI-TP84/13, 1984 (unpublished).
[10]K. Kajantie, Phys. Lett. **65B**, 69 (1976).
[11]J. Badier *et al.*, Phys. Lett. **142B**, 446 (1984).
[12]T. Ferbel and W. R. Molzon, Rev. Mod. Phys. **56**, 181 (1984); H. Specht, in *Quark Matter '84,* proceedings of the Fourth International Conference on Ultrarelativistic Nucleus-Nucleus Collisions, Helsinki, 1984, edited by K. Kajantie (Springer, New York, 1985).
[13]G. Baym, in *Quark Matter '84* (Ref. 12).
[14]J. D. Bjorken, Phys. Rev. D **27**, 140 (1983).
[15]M. Gyulassy and T. Matsui, Phys. Rev. D **29**, 419 (1984).
[16]G. Baym, B. Friman, J.-P. Blaizot, and M. Soyeur, Nucl. Phys. **A407**, 541 (1983).
[17]E. V. Shuryak and O. V. Zhirov, Phys. Lett. **89B**, 253 (1979).
[18]L. Van Hove, Phys. Lett. **118B**, 138 (1982).
[19]Y. Hama and F. S. Navarra, Phys. Lett. **129B**, 251 (1983).
[20]M. Gyulassy, Nucl. Phys. **A418**, 59C (1984).
[21]A. Capella, C. Pajares, and A. V. Ramallo, Nucl. Phys. **B241**, 75 (1984).
[22]I. Otterlund, S. Garpman, I. Lund, and E. Stenlund, Z. Phys. C **20**, 281 (1983).
[23]P. Landshoff and J. Polkinghorne, Nucl. Phys. **B33**, 221 (1971).
[24]J. D. Bjorken and H. Weisberg, Phys. Rev. D **13**, 1405 (1976).
[25]V. Černý, P. Lichard, and J. Pišút, Phys. Lett. **70B**, 61 (1977).
[26]J. K. Yoh *et al.*, Phys. Rev. Lett. **41**, 684 (1978).
[27]F. Halzen and P. Hoyer, Phys. Lett. **130B**, 326 (1983).
[28]B. Combridge and C. Maxwell, Nucl. Phys. **B239**, 429 (1984).
[29]R. Gandhi, F. Halzen, and F. Herzog, Phys. Lett. **152B**, 261 (1985).
[30]A. Aurenche, A. Douiri, R. Baier, M. Fontannaz, and D. Schiff, Phys. Lett. **140B**, 87 (1984).
[31]Roland Svensson, Astrophys. J. **258**, 321 (1982); **258**, 335 (1982), and references cited therein.
[32]V. V. Klimov, Zh. Eksp. Teor. Fiz. **82**, 336 (1982) [Sov. Phys. JETP **55**, 199 (1982)].
[33]K. Kajantie and P. V. Ruuskanen, Phys. Lett. **121B**, 352 (1983).
[34]C. Quigg, Astrophys. J. **151**, 1187 (1968).
[35]G. Baym, Phys. Lett. **138B**, 18 (1984).
[36]R. C. Hwa, Phys. Rev. D **32**, 637 (1985).